

THE RELATIVE ROLE OF GALAXY MERGERS AND COSMIC FLOWS IN FEEDING BLACK HOLES

JILLIAN BELLOVARY¹, ALYSON BROOKS², MARTA VOLONTERI³, FABIO GOVERNATO⁴, THOMAS QUINN⁴, JAMES WADSLEY⁵

Draft version October 11, 2018

ABSTRACT

Using a set of zoomed-in cosmological simulations of high-redshift progenitors of massive galaxies, we isolate and trace the history of gas that is accreted by central supermassive black holes. We determine the origins of the accreted gas, in terms of whether it entered the galaxy during a merger event or was smoothly accreted. Furthermore, we designate whether the smoothly accreted gas is accreted via a cold flow or is shocked upon entry into the halo. For moderate-mass ($10^6 - 10^7 M_{\odot}$) black holes at $z \sim 4$, there is a preference to accrete cold flow gas than gas of shocked or merger origin. However, this result is a consequence of the fact that the entire galaxy has a higher fraction of gas from cold flows. In general, each black hole tends to accrete the same fractions of smooth- and merger-accreted gas as is contained in its host galaxy, suggesting that once gas enters a halo it becomes well-mixed, and its origins are erased. We find that the angular momentum of the gas upon halo entry is a more important factor; black holes preferentially accrete gas that had low angular momentum when it entered the galaxy, regardless of whether it was accreted smoothly or through mergers.

Subject headings: galaxies: formation, galaxies: evolution, black hole physics, galaxies: high-redshift, methods: numerical

1. INTRODUCTION

The classic model for fueling bright quasars at high redshift assumes that massive black holes (MBHs) are powered by major galaxy mergers, which cause large quantities of gas to be funneled into the regions where MBHs reside (e.g. Kauffmann & Haehnelt 2000; Haiman & Loeb 2001; Di Matteo et al. 2005; Hopkins et al. 2006; Li et al. 2007; Sijacki et al. 2009). The result of this process is near-simultaneous bursts of star formation and MBH accretion, which are observed at all redshifts in a large range of galaxy types. Indeed, the peaks in global star formation and quasar activity coincide at a redshift of $\sim 2 - 3$ (Hopkins 2004; Richards et al. 2006; Reddy et al. 2008), which strengthens the argument that these two phenomena must be connected. Observations support this picture, with growing numbers of observed high-redshift galaxies exhibiting both powerful star formation and active galactic nucleus (AGN) activity (Alexander et al. 2005; Papovich et al. 2006; Menéndez-Delmestre et al. 2007; Silverman et al. 2009; Coppin et al. 2010; Mullaney et al. 2012; Kirkpatrick et al. 2012; Chen et al. 2013). Nearby massive early-type quasar host galaxies are also observed to exhibit signs of a recent major merger (Sanders et al. 1988; Disney et al. 1995; Bahcall et al. 1997; Canalizo & Stockton 2001; Hutchings et al. 2003; Guyon et al. 2006; Bennert et al. 2008; Urrutia et al. 2008; Wolf & Sheinis 2008; Tal et al.

2009; Schawinski et al. 2010). A popular suggested paradigm involves a gas-rich major merger triggering a burst of star formation, channeling gas into the central regions of the galaxy, and fueling a powerful AGN. The energy released by accreting gas may unbind the remaining gas from the galaxy, rendering the galaxy “red and dead” and eventually resembling today’s massive ellipticals (Di Matteo et al. 2005; Hopkins et al. 2006).

However, there is also evidence for AGN activity that is not necessarily merger-driven. Low to moderate luminosity AGN hosts tend to be disk-dominated at high redshifts (Schawinski et al. 2011; Kocevski et al. 2012) and in the local universe (e.g. De Robertis et al. 1998). Recently, Treister et al. (2012) postulated that major mergers are the primary drivers of accretion in only the most luminous AGN. Furthermore, they suggest that this trend does not appear to evolve with redshift; moderate-luminosity AGN inhabit quiescent galaxies out to $z \sim 2 - 3$.

Locally, low-luminosity AGN hosts tend to be disk galaxies, which are unlikely to have undergone a recent major merger. Recent studies have examined MBH fueling in local AGN and found that gravitational torques are efficient at transporting gas from the galactic disk to the central region (Haan et al. 2009; García-Burillo et al. 2005). Ryan et al. (2007) examined a sample of narrow-line Seyfert 1 galaxies and found no evidence for merger events, tidal tails, or disrupted features. The lack of merger-induced features for these galaxies is a hint that their black hole growth is driven by secular processes rather than interactions with other galaxies. Furthermore, Hicks et al. (2013) demonstrate that in a matched sample of Seyfert and quiescent galaxies, AGN hosts are more centrally concentrated with a larger reservoir of molecular gas, perhaps indicating that active nuclei have simply experienced recently triggered inflowing material.

In addition to secular processes, and especially at

¹ Department of Physics and Astronomy, Vanderbilt University, Nashville, TN

² Department of Astronomy, University of Wisconsin-Madison, Madison, WI

³ IAP, Paris, France

⁴ Department of Astronomy, University of Washington, Seattle, WA

⁵ Department of Physics and Astronomy, McMaster University, Hamilton, ON, Canada

high redshifts, MBHs may be fueled by gas which is directly accreted onto a galaxy from the intergalactic medium. These “cold flows” may take the form of filamentary inflows, especially at high redshift (Binney 1977; Kereš et al. 2005; Dekel & Birnboim 2006; Ocvirk et al. 2008). Such flows fueling MBH growth have been demonstrated in large volume and high resolution cosmological simulations (Di Matteo et al. 2012; Dubois et al. 2012, respectively). The role of cold flows on MBH growth may be significant among the most massive rare halos, but the effect on more common, less massive halos has yet to be investigated, and is the primary goal of this paper.

The diversity of AGN hosts suggests that there exists a diversity of fueling mechanisms. For instance, while not all AGN activity is merger driven, mergers or interactions seem to enhance AGN activity (Silverman et al. 2011). Properties such as galaxy/halo mass, merger history, gas accretion history, and environment likely all play a role in when and how much MBHs accrete. Thus, the aforementioned paradigm of major mergers fueling MBH growth is likely only a dominant mechanism for a small subset of highly luminous objects. The question “how do MBHs grow?” is likely a very complex one for black holes in different environments. To address one aspect of this question, we focus on late-type galaxies at $z = 4$ which host moderate-luminosity AGN. The advantage of studying MBH growth in cosmological simulations is that one can disentangle effects from major galaxy mergers as well as accretion of ambient cold gas from cold flows/filaments, minor mergers, and secular evolution.

In this work we separate accretion by mergers and the ambient environment by tracing the history of every gas particle as it enters the primary halo. Furthermore, we differentiate between cold flows and gas which is shocked upon entering the virial radius of the halo. We then trace each gas particle on its way to being accreted by the central MBH. In section 2 we describe the simulations used in our study. Section 3 describes the method used to trace the history of the gas particles. In section 4 we reveal the role of the origins of gas as well as its angular momentum in fueling central MBHs. We leave studies of minor mergers and secular processes to a future work, and summarize our results in section 5.

2. THE SIMULATIONS

We have run our cosmological simulations using the Smoothed Particle Hydrodynamics N -Body Tree code Gasoline (Stadel 2001; Wadsley et al. 2004). Gasoline includes prescriptions for star formation and supernova feedback (Stinson et al. 2006), metal diffusion (Shen et al. 2010), and massive black hole formation, accretion, and feedback (Bellovary et al. 2010). All of our simulations use a Kroupa IMF (Kroupa 2001), WMAP3 cosmology (Spergel et al. 2007), and a uniform UV background (Haardt & Madau 1996). Galaxies simulated with Gasoline have been shown to lie on the observed Tully-Fisher relation (Governato et al. 2009), the mass-metallicity relation (Brooks et al. 2007), the size-luminosity relation (Brooks et al. 2011), and have realistic baryon fractions and matter distributions (Governato et al. 2010; Guedes et al. 2011). Our simulations use primordial cooling plus a low-temperature

extension to the cooling curve due to trace metals (Bromm et al. 2001). While we do not include cooling via metals or molecular hydrogen, gas is allowed to reach a minimum temperature of $\sim 100\text{K}$. The abovementioned works demonstrate that we are able to simulate realistic galaxies without the addition of these advanced features (see also Christensen et al. 2012). While these previous results have not included the effects of AGN feedback, our current studies suggest that for galaxies of small to moderate masses (such as those studied previously and in this work) the central SMBH affects only the central regions of the galaxies and leaves the more global properties intact; we are thus confident that the simulations presented in this paper are quite consistent with the broad range of observed galaxy properties.

We have selected three halos of interest from a uniform volume of size 50 Mpc, and re-simulated each of them individually using the volume renormalization technique (Katz 1992). The selected galaxies are the progenitors of today’s massive ellipticals, with $z = 0$ virial masses of between $1 - 9 \times 10^{13}$; however, we have chosen to maximize resolution and evolve these galaxies only until redshift $z \sim 4$. The force resolution is 260 comoving pc, and the gas and dark matter particle masses are $9 \times 10^4 M_\odot$ and $1.3 \times 10^5 M_\odot$ respectively. Table 1 describes the properties of the simulations at $z = 4$ in detail, including the number of particles within the virial radius, the virial mass, maximum value of the circular velocity, virial radius (defined as the radius in which the enclosed density is 200 times that of the critical density of the universe at $z=4$), and stellar disk scale radius as measured with an exponential profile.

Star formation is modeled stochastically, with gas particles becoming eligible to form stars if they are above the density threshold (2.5 amu cm^{-3}) and below the temperature threshold (10^4 K). We use a star formation efficiency parameter of $c^* = 0.1$, and a supernova feedback energy of $E_{SN} = 8 \times 10^{50} \text{ erg}$. This energy is distributed to particles within a radius determined by the blastwave equations of McKee & Ostriker (1977); the heated particles have their cooling disabled for a timescale also determined by these equations. This combination of parameter choice and resolution results in galaxies which are consistent with the stellar mass - halo mass relation (Moster et al. 2010; Munshi et al. 2013) at $z \sim 4$ (Figure 1) and have realistic star formation histories. Thus, while there are few observational structural constraints at $z = 4$ for late-type galaxies, we are confident that we can adequately represent galaxy and MBH growth at this epoch.

Seed black hole formation is also stochastic, and is similar to star formation with the additional requirement that black holes must form out of zero-metallicity gas. If a gas particle meets the criteria for star formation and additionally has zero metallicity, it has an additional probability, χ_{seed} , that it will instead form a black hole with mass equal to the mass of the parent gas particle ($9 \times 10^4 M_\odot$). For our simulations here we set $\chi_{seed} = 0.2$, which achieves reasonable MBH occupation fractions in galaxies without overproducing MBH-MBH merger events (which results in MBHs which violate the Soltan argument, growing almost solely through mergers and not gas accretion). This requirement is

TABLE 1
SIMULATION PROPERTIES

Run	# within R_{vir}	M_{vir} (M_{\odot})	M_{gas} (M_{\odot})	M_{star} (M_{\odot})	V_{max} (km/s)	R_{vir} (kpc)	r_s (kpc)
hz2	2758081	2.52×10^{11}	2.36×10^{10}	1.63×10^{10}	267	196	2.39
hz3	3516774	3.17×10^{11}	3.62×10^{10}	2.06×10^{10}	190	211	2.51
hz4	527952	5.81×10^{10}	7.53×10^9	9.64×10^8	106	120	0.80

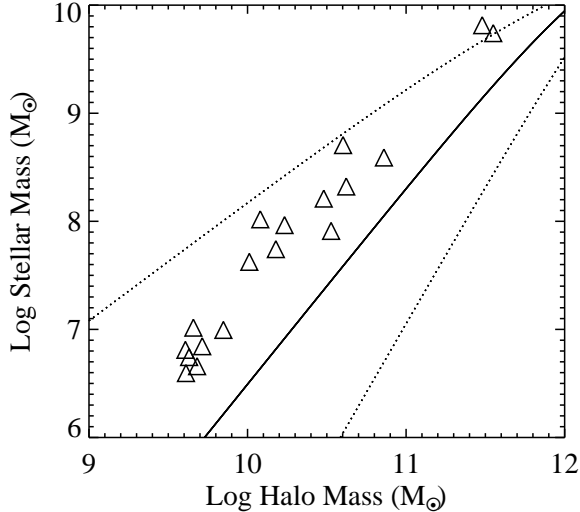


FIG. 1.— The stellar mass - halo mass relation for every single galaxy with more than 20,000 dark matter particles in all three simulations at $z = 4$. The solid line is the analytical relation derived for $z = 3.5$ and the dotted lines encompass the $1-\sigma$ errors for that relation (Moster et al. 2010).

broadly consistent with theories of seed black hole formation out of Population III stars (Couchman & Rees 1986; Abel et al. 2002; Bromm & Larson 2004) or direct collapse of gas (Loeb & Rasio 1994; Eisenstein & Loeb 1995; Koushiappas et al. 2004; Begelman et al. 2006; Lodato & Natarajan 2006). It also ensures that seed black holes cease forming at high redshift, once the interstellar medium becomes polluted with metals from supernova feedback. Multiple black holes may form in a single halo; additionally, they are not fixed to halo centers but are allowed to react dynamically to perturbations such as galaxy mergers. In order to decrease the effects of artificial two-body scattering, we employ dark matter particle masses that are only slightly larger than the black hole masses, which helps the black holes stay in the centers of their hosts. For more details on seed black hole formation, see Bellovary et al. (2011).

Black holes are allowed to merge if they (a) are within twice one another’s softening length and (b) fulfill the criterion $\frac{1}{2}\Delta\vec{v}^2 < \Delta\vec{a} \cdot \Delta\vec{r}$, where $\Delta\vec{v}$ and $\Delta\vec{a}$ are the differences in velocity and acceleration of the two MBHs, and $\Delta\vec{r}$ is the distance between them. Black holes also grow through gas accretion, via the Bondi-Hoyle method:

$$\dot{M} = \frac{4\pi\alpha G^2 M_{BH}^2 \rho}{(c_s^2 + v^2)^{3/2}} \quad (1)$$

where ρ is the density of the nearby gas, c_s is the sound speed, v is the relative velocity of the black hole to the gas, and α is a constant equal to 1. Feedback energy is

imparted on the surrounding gas and is proportional to the accretion rate:

$$\dot{E} = \epsilon_r \epsilon_f \dot{M} c^2 \quad (2)$$

assuming $\epsilon_r = 0.1$ as the radiative efficiency, and $\epsilon_f = 0.03$ as the efficiency at which the feedback energy, which is distributed over the SPH kernel as thermal energy to the 32 particles nearest the black hole, couples to the gas. Other groups often use a value of $\epsilon_f = 0.05$ (e.g. Sijacki et al. 2007; Di Matteo et al. 2008); however, we find that using this higher value results in overpowered feedback and very limited gas accretion. Using $\epsilon_f = 0.03$ results in MBHs which match the observed MBH-host galaxy scaling relations, such as $M_{BH} - \sigma$ and $M_{BH} - M_{bulge}$ (e.g. Figure 2). Since this number is not meant to represent a precise physical quantity, but is merely a parameter used in subgrid feedback models in simulations, slight differences among various codes are expected. In addition, in this work we are examining the relative contribution of various channels of gas accretion rather than an absolute value of accreted gas mass, and thus our results are not highly dependent on our feedback implementation.

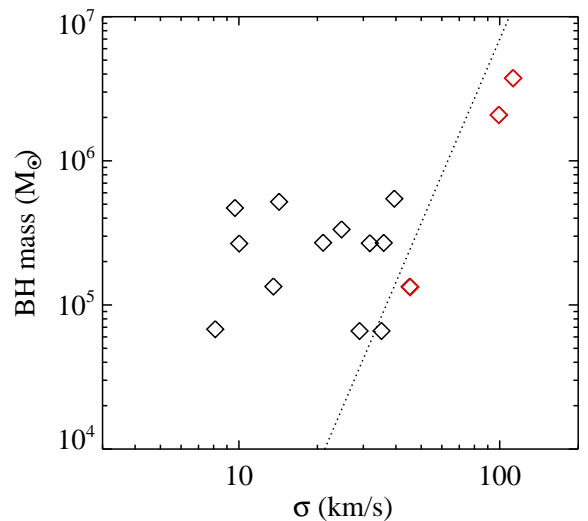


FIG. 2.— The $z = 4$ $M-\sigma$ relation for galaxies in all three simulation boxes. The three central galaxies are highlighted in red. The dotted line is the local relation derived by Gültekin et al. (2009). The “plume” of massive objects at low σ is a result of our relatively massive MBH seeds (see Volonteri & Natarajan 2009).

3. TRACING GAS ACCRETION

The following section is a summary of the methodology described in Brooks et al. (2009), which is a comprehensive study of how galaxies accrete gas in cosmological

simulations. While the focus of Brooks et al. (2009) is on the gaseous and stellar buildup of galaxy disks, the gas-tracing methodology can be applied to many scenarios, including the accretion of gas by black holes.

Galaxies are identified using the Amiga Halo Finder (AHF; Knebe et al. 2001; Gill et al. 2004; Knollmann & Knebe 2009), which identifies a virial radius based on the overdensity criterion for a flat universe (Gross 1997). Before their accretion onto the primary halo, gas particles are traced to determine if they ever belonged to a halo other than the primary. To define the primary halo, we identify the central MBH of the most massive galaxy at the final step of the simulation. We then trace this MBH back in time and identify its host as the primary at each step.

If gas particles are already in the primary halo at the first step where halos are identified ($z = 15$ in this study), they are labeled as “early” accretion. Gas particles that have ever belonged to any halo or subhalo other than the primary halo are labeled as “clumpy” accretion, and are generally accreted onto the main galaxy in merger events. Gas that enters the halo in any other fashion is labeled “smooth” accretion, which is then divided into two categories, cold and shocked.

Smoothly accreted gas particles may or may not undergo a shock within the virial radius of the primary galaxy (Dekel & Birnboim 2006; Kereš et al. 2009; van de Voort et al. 2011). The presence of a shock depends mainly on the mass of the halo; generally, gas will shock if the galaxy halo is around $10^{11} M_{\odot}$ (Ocvirk et al. 2008). Thus, since dwarf galaxies are less massive than this threshold, they will never develop a shock. In massive galaxies, the development of a shock is strongly related to the orientation of the gas flow. Cold gas predominantly flows into halos along the filaments inherent to the large-scale structure of the universe, and these filaments may be dense enough to penetrate a shock front and deliver gas to the central galaxy without heating the gas to the virial temperature (Kereš et al. 2009; Dekel et al. 2009; Brooks et al. 2009; Stewart et al. 2011; van de Voort et al. 2011; Stewart et al. 2013). Eventually the filaments dissipate, but for a substantial time these filaments are critical in building up galaxy disks at high redshift (Brooks et al. 2009; Pichon et al. 2011; Danovich et al. 2012).

Shocked gas by definition undergoes an entropy increase, which also manifests as a temperature increase. Thus, gas is identified as shocked if it increases its entropy and density based on these two criteria (see also Dekel & Birnboim 2006):

$$T_{shock} \geq 3/8 T_{vir}, \quad (3)$$

where T_{vir} is the virial temperature of the halo, and

$$\Delta S \geq S_{shock} - S_0, \quad (4)$$

where S_0 is the initial entropy of the gas particle and

$$S_{shock} = \log_{10}[3/8 T_{vir}^{1.5}/4\rho_0] \quad (5)$$

where ρ_0 is the gas density prior to encountering the shock. Smoothly accreted gas is traced until it reaches a distance of $0.1R_{vir}$ from the galaxy; after this point,

supernova feedback can mimic the effects of virial shocking, which can no longer be accurately tracked. Any smoothly accreted gas particle that undergoes the above temperature and entropy increases is defined as shocked. Those gas particles that reach $0.1R_{vir}$ without these increases is defined as unshocked (repeating the calculation for tracking radii larger than $0.1R_{vir}$ gives no substantial difference in our results). We refer the reader to Brooks et al. (2009) for more complete details of the relevant shock physics.

Armed with these categories of gas accretion, we determine how MBHs accrete their own gas. We identify the gas particles which are accreted by the primary MBH in a simulation (defined as the MBH residing at the center of the primary galaxy). We then cross-correlate these particles with their accretion history. This process provides a history for the accreted gas particles as they enter the primary galaxy, though does not give any information about which mechanisms govern their journey to the MBH. This information must be gleaned in further analysis.

4. HOW DO BLACK HOLES GET THEIR GAS?

Figure 3 shows simulated SDSS *gri* images of the primary galaxies in each simulation, which were created with Sunrise (Jonsson 2006). The images show blue colors and late-type morphologies for all three galaxies. Our three chosen simulations have similar mass and environment. They each form in gas-rich filaments and accrete gas from this cold flow as well as through galaxy mergers. However, they have a variety of merger histories; for example, the largest galaxy (*hz2*) has an active history, undergoing a few major mergers (defined as mergers with stellar mass ratio 1:3 or larger). The galaxies *hz3* and *hz4* are somewhat more quiescent, with mostly minor mergers (stellar mass ratio between 1:3 and 1:10). We have chosen these simulations in order to examine how galaxies with different interaction histories may experience different MBH growth. In Figure 4 we show the bolometric luminosity vs time for the central MBH in the primary galaxy for each simulation. We highlight major merger events with red hatched regions, and minor mergers with blue hatching. Mergers are defined to begin when the satellite enters the primary’s virial radius, and end when the satellite is disrupted. While each lightcurve is fairly noisy, mergers do not seem to substantially enhance the fueling of low-mass MBHs. However, major mergers trigger strong AGN activity only after the third pericenter passage, when central MBHs are ~ 1 kpc apart (Van Wassenhove et al. 2012), and our resolution limits our ability to analyze this phase in great detail. At lower redshifts there are several extremely minor mergers (with ratios less than 1:10) as well as a variety of secular instabilities which occur during each galaxy’s evolution; the MBH appears to undergo at least as many spurts of growth during these episodes as during more substantial mergers. The MBH in *hz2* reaches a bolometric luminosity greater than $10^{42} \text{ erg s}^{-1}$ for a duration of 66 Myr, or 4.5% of its lifetime, and exceeds a luminosity of $10^{43} \text{ erg s}^{-1}$ for a total of 3.7 Myr. The MBH in *hz3* spends 15 Myr (1% of its lifetime) at a luminosity greater than $10^{42} \text{ erg s}^{-1}$. The MBH in *hz4* experiences very little growth by accretion. The luminosities of the MBHs in *hz2* and *hz3* are comparable to those of nearby Seyfert

galaxies, but are unobservable at the high redshifts of our simulations.

We show the growth of the primary black hole in the largest galaxy in each run in Figure 5. Each MBH begins with a seed mass of $9 \times 10^4 M_{\odot}$, and subsequently grows through merging with other MBHs and via gas accretion. The purple dashed line indicates the total MBH mass, including the initial seed mass and growth through MBH mergers. The solid black line represents the total mass gained by gas accretion only. The colored solid lines show the mass due to gas accretion divided into each accretion mode: unshocked/cold flows (blue), shocked (red), and clumpy (green).

In each galaxy, we see that gas which originated in cold flows dominates the MBH accretion. This result indicates that gas from other galaxies does not always travel directly to the central MBH during mergers, but may get mixed into the host galaxy’s gas reservoir, or delayed in entering the central regions due to an elongated orbit. Cold flow gas appears to be the dominant fuel for MBHs; we must investigate whether this result is due to cold flows being more efficient MBH feeders, or whether they simply provide the most gas to their host galaxies.

4.1. Gas Fractions

While Figure 5 gives insights on the mode of gas which is accreted by MBHs, it does not give us any information on whether one mode is preferentially accreted over another. To do this, we must compare the fraction of each mode accreted by the MBH to the fraction of each mode that composes our entire galactic halo. If a halo is comprised of gas hailing from one particular mode of accretion, it follows that the MBH will also accrete the majority of its gas from the same mode. On the other hand, if the modal fractions accreted by the MBH are different from those comprising the overall galaxy, we can clarify whether one mode is preferentially accreted over another.

Table 2 shows the fractions of unshocked, clumpy, and shocked gas accreted by the galaxy and MBH for each of the three simulations. The “stars” column is the fraction of stellar mass which formed in-situ from gas originating in each accretion mode (stars which formed in another galaxy are not included). For simulation *hz4*, the primary is never large enough to host a shock. The remainder of the gas in *hz4* is classified as “early” accretion: gas which was already in the galaxy at $z = 15$. For *hz2* and *hz3* the early fraction is negligible.

Cold flows are generally the dominant source of accretion for both the overall galaxy and the central MBH, followed by gas from mergers. Overall, there is very little difference between the modal fractions of accreted gas for the galaxies and the MBHs. The stars, on the other hand, seem to show a very slight relative preference to form from merger gas compared to the MBH’s preference for unshocked gas (in relation to the overall galaxy composition). While a detailed study of this phenomenon is beyond the scope of this paper, we suspect that gas entering the main galaxy during a merger may experience a variety of processes which may cause it to form stars; on the other hand, to feed the MBH it must be channeled to a specific location. We stress that while these trends are evident for all three galaxies in our sample, the differences are only a few percent. Overall, each

black hole tends to accrete more or less the same fractions of smooth- and merger-accreted gas as is contained in its host galaxy.

We explore the evolution of these gas fractions with redshift in Figure 6. The dashed lines show the instantaneous fraction of gas mass accreted by the MBH in *hz2* for each accretion mode, while the solid lines show the gas fraction of the galaxy as a whole (colors are as in Figure 5, with the addition of gray lines representing “early” gas which is within the galaxy at the beginning of the tracing history). High- z mergers, which occur in *hz2*’s history around $z \sim 7 - 10$, have the result of dumping a large quantity of gas into the host galaxy, which also increases the fraction the MBH accretes fairly instantaneously. Such behavior is evidence of mergers directly fueling MBH growth at high redshift. On the other hand, at times when the galaxy’s accretion as a whole becomes more cold-flow-dominated, the MBH also tends to increase the fraction of cold-flow-originated gas it accretes. The general trend is that the modal fraction which the MBH accretes is merely whatever is available in the galaxy, with a slight delay in time while the MBH’s fuel reservoir adjusts to the composition of the entire system. (While we show this figure for simulation *hz2*, the results for *hz3* and *hz4* are qualitatively similar.)

To focus on the galaxy center, which is the residence of the MBH, in Figure 7 we plot the mass fractions of newly formed stars within the central 500 parsecs, categorized by the origins of the gas from which they formed. For each simulation output (roughly 50 Myr apart), we determine which stars have formed in the central region since the previous timestep. In addition we sum the gas mass accreted by the MBH during these same timesteps. These differential mass fractions of stars and accreted gas show that the fractions of gas which are accreted by the MBH are slightly different than the fractions which result in newly formed stars at each timestep. The MBH accretes a higher fraction of cold flow gas throughout its history compared to the composition of the stars which form at the same time in the same region, and a lower fraction of clumpy and shocked gas. However, these fractions are still within 10 – 20% of each other at all times. Broadly speaking, the origins of accreted gas which comprise up the overall gaseous, stellar, and MBH makeup in a galaxy are consistent within this factor. Thus, *at any given time, the accretion history of the MBH will resemble the accretion history of the galaxy; if we can untangle a galaxy’s history, we can assume it for the MBHs as well.*

4.2. Angular Momentum

Since the accretion origin of gas does not play a major role in what a MBH preferentially accretes, one might ask what process *does* play a role in feeding central black holes. One possibility is the angular momentum of the inflowing gas; gas with low angular momentum is more likely to travel directly to the galaxy center instead of getting caught up in a rotating disk. To study how the angular momentum of accreted gas may affect how it is accreted by the MBH, we have measured this quantity for every gas particle at the moment when it enters the primary halo. For smoothly accreted gas, this moment is when the particle crosses the virial radius; for clumpy gas, the moment is when the gas can no longer be iden-

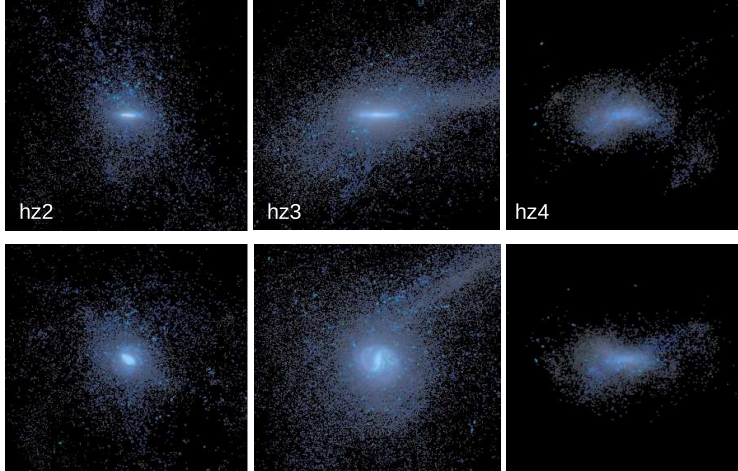


FIG. 3.— Edge-on (top row) and face-on (bottom row) of the primary galaxies in simulations *hz2*, *hz3*, and *hz4* (left, center, and right, respectively). Images are unreddened SDSS *gri* composites created with Sunrise (Jonsson 2006) and are 30 kpc on a side. The rest-frame unreddened absolute magnitudes in the *Hubble* ACS F435 band are -23.6, -24.0, and -20.9, respectively.

TABLE 2
GALAXY VS. MBH ACCRETION

Gas Origin	hz2			hz3			hz4		
	gas	stars	MBH	gas	stars	MBH	gas	stars	MBH
Unshocked	62%	60%	66%	50%	42%	47%	65%	58%	47%
Clumpy	25%	28%	21%	30%	35%	28%	30%	35%	28%
Shocked	13%	12%	14%	20%	23%	25%	0%	0%	0%

tified with its host galaxy (at which point it may have spent several timesteps within R_{vir}). In Figure 8, we plot the normalized cumulative distribution of specific angular momenta for each gas particle as it enters the primary galaxy in simulation *hz2* (our results are similar for simulations *hz3* and *hz4*). The colored lines represent the various gas accretion modes onto the halo, as in Figure 5. The solid lines represent the entire gas content of the halo, while the dashed lines are only the gas which is eventually accreted by the central MBH. Gas originating in mergers has markedly less angular momentum overall. This finding may be a result of our definition of the moment when gas enters the halo, which is different for clumpy and smoothly accreted gas (although for evidence that cold flows carry greater angular momentum see Kimm et al. (2011) and Stewart et al. (2013)). This result is fairly intuitive - smoothly accreted gas may be torqued by the existing gas halo on its way to the primary galaxy (Roškar et al. 2010; Dubois et al. 2012; Tillson et al. 2012), but gas entering in satellite halos will be able to continue on the original trajectory of its satellite and initially avoid these strong torques. At early times, these satellites tend to fall in along the filaments (Benson 2005), with fairly radial orbits resulting in early head-on collisions with the primary.

Gas with lower initial angular momentum will reach the galaxy center more efficiently and thus be more likely to feed the MBH. Comparing the solid and dashed lines, in each case the gas which is accreted by the MBH has overall lower angular momentum than that of the over-

all gas distribution. While a loss of angular momentum is required for MBH accretion, there is not a clear argument that one mode of accretion is more efficient at losing angular momentum than another. This result strengthens our argument that the accretion origin of the gas is not the primary driver behind how MBHs grow, but rather the incoming angular momentum determines its likelihood for feeding an MBH.

5. SUMMARY

We have performed an extensive study of the origins of gas accreted by high- z MBHs in full cosmological simulations. We trace the history of the gas particles and categorize them in terms of smooth accretion or accretion in mergers, i.e. “clumpy.” The smoothly accreted gas is further divided into shocked and unshocked categories, based on their temperature and entropy histories as they enter the primary halo. We simulate three massive galaxy progenitors to redshift $z = 4$. We study the gas accretion history for these individual galaxies and their primary MBHs to determine which gas is accreted most efficiently and eventually fuels low-luminosity AGNs.

While our MBHs are predominantly fed by cold flows, this result is an effect of the composition of the galaxy and not because cold flows are a preferred method of accretion. MBHs are not picky; they will accrete whatever gas their host galaxy provides. The previous study by Di Matteo et al. (2012) reports several MBHs in a simulated volume growing by accretion from cold flows; however, this gas was identified by temperature only, and

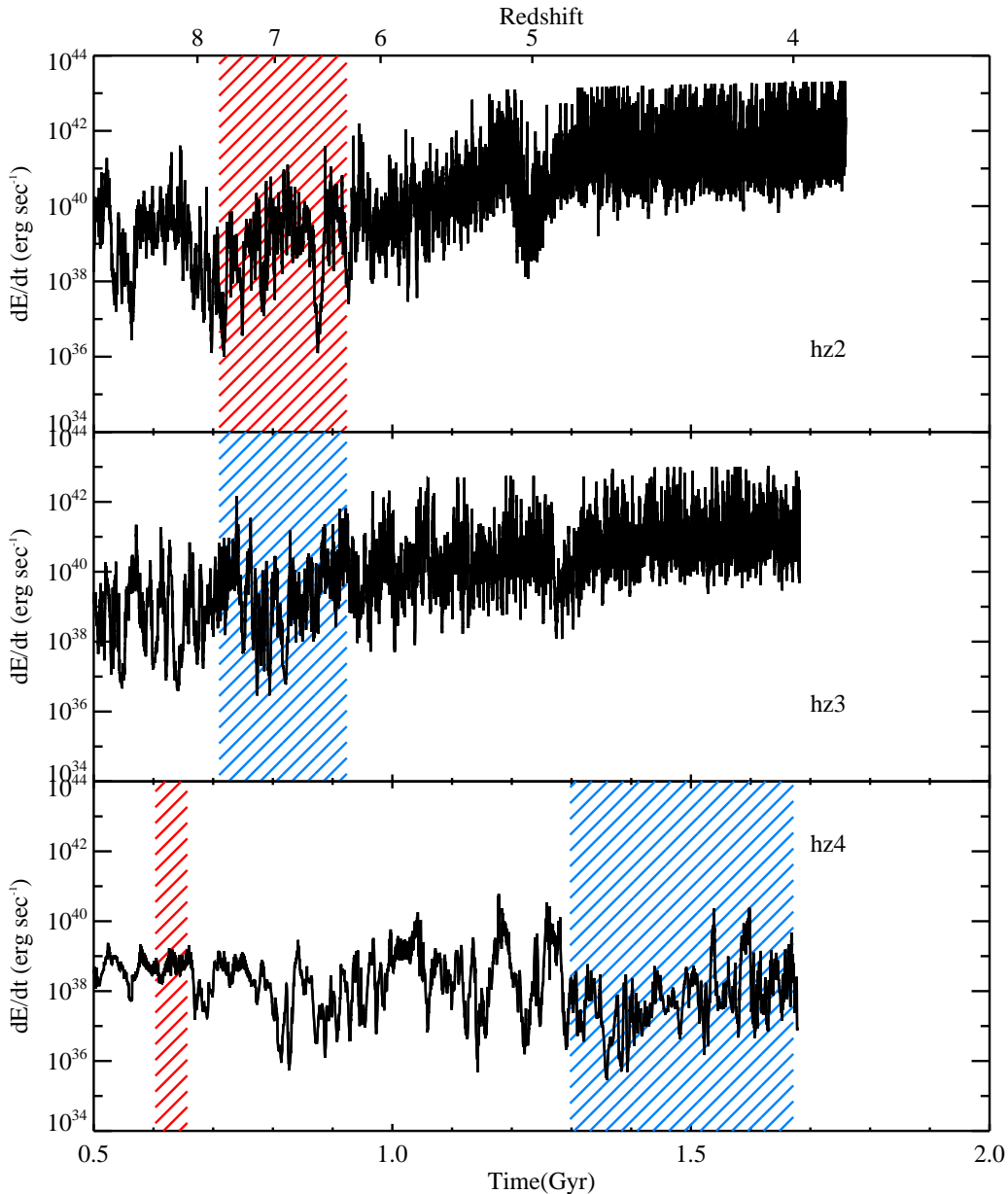


FIG. 4.— Bolometric luminosity from accretion onto the primary MBH vs time for the most massive galaxy in *hz2* (top), *hz3* (middle), and *hz4* (bottom). Major mergers are marked with a red hatched region, and minor mergers with a blue hatched region. Merger events do not substantially affect the growth of these lower mass MBHs.

not whether it was accreted smoothly or in mergers. The authors report that few major mergers take place; by default, the host galaxy’s gas must consist primarily of smoothly accreted gas. The MBHs in their work as well as our own grow via cold flows because they exist in a galaxy which is fed by cold flows, not necessarily because cold flows preferentially feed MBHs.

We find that angular momentum is a more fundamental factor in determining the origins of gas which grows MBHs. Our findings agree with those of Dubois et al. (2012), who report efficient feeding of central MBHs via low angular momentum cold streams. In addition, they find that larger mass halos have an increased fraction of radially infalling gas. A broader picture is emerging; more massive halos (which form earlier than low-mass halos, (e.g. Bower et al. 2006)) exhibit large amounts of

low angular momentum gas, which can efficiently fuel bright quasars and star formation at high redshift (see also Dubois et al. 2013). On the other hand, the angular momentum content of later-collapsing gas is higher, since it is torqued for a longer period of time. Additionally, lower mass galaxies eject low angular momentum gas via feedback processes more efficiently (Governato et al. 2010; Brook et al. 2011) due to their shallower potential wells. Therefore moderate-mass halos host lower luminosity AGN, fueled less efficiently because the available gas has too much inherent spin.

The evidence for merger activity fueling MBH growth is plentiful, but does not present a full picture. While bright quasars are certainly present in the remnants of gas-rich major mergers, we have shown that MBH fueling at high redshift can occur in a number of ways, and

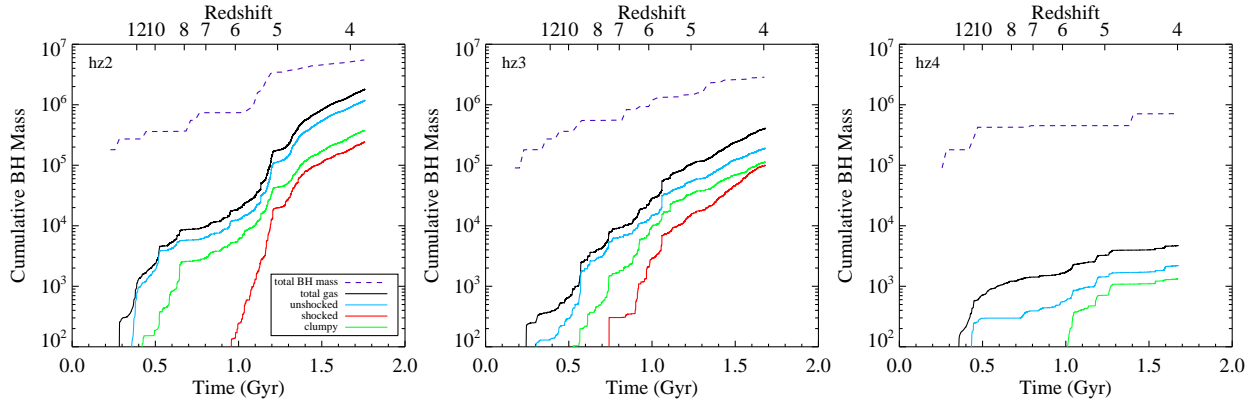


FIG. 5.— Growth of the primary MBH in the the largest galaxy in simulation *hz2* (left), *hz3* (center), and *hz4* (right). The upper dashed line is the total mass of the MBH. The solid black line is the total resulting from accreted gas. The blue, green, and red lines represent accreted gas originating from unshocked flows, mergers, and shocked accretion, respectively.

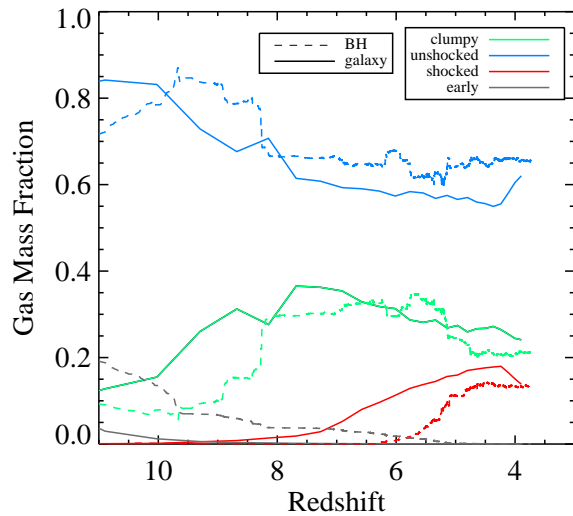


FIG. 6.— Cumulative gas fractions vs redshift for the primary galaxy in simulation *hz2*. Colors are as in Figure 5, with the addition of a gray line representing gas which is within the galaxy at the beginning of the tracing history. Solid lines represent entire halo fractions, dashed lines represent MBH fractions.

reflects the gas accretion history of the host galaxy. Even so, we have just begun to explore the full parameter space of galaxy mass, redshift, gas content, and merger history, and how these quantities affect MBH growth. Additionally, the journey of the gas from the outer edge of the halo to the central MBH is still enigmatic. Torques from mergers and secular processes drive gas inwards, fueling the black hole, but how and when this occurs will be the focus of further study.

Simulations were run using computer resources and technical support from NAS. JB acknowledges support from NSF CAREER award AST-0847696, as well as support from the Aspen Center for Physics. MV acknowledges funding support from NASA, through Award

Number ATP NNX10AC84G; from SAO, through Award Number TM1-12007X, from NSF, through Award Number AST 1107675, and from a Marie Curie Career Integration grant (PCIG10-GA-2011-303609). FG acknowledges support from a NSF grant AST-0607819 and NASA ATP NNX08AG84G. JB and TQ acknowledge support from NASA Grant NNX07AH03G. AB acknowl-

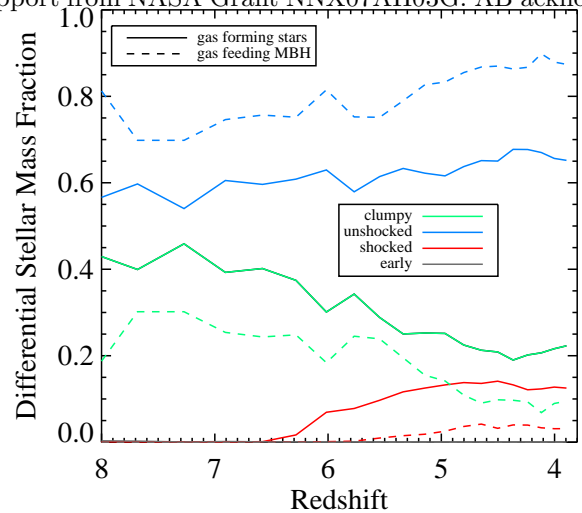


FIG. 7.— Differential stellar mass fraction and MBH accretion fraction vs redshift for *hz2*. Colors are as in Figure 6. In time bins of ~ 50 Myr, we determine the accretion origin of the gas which has recently formed stars within the central 500 (physical) parsecs (solid lines) and compare the mass fractions to the mass fractions which the MBH accretes (dashed lines) in that same time range. In each case the modal fraction of gas accreted by the MBH follows that of the galaxy, in a general sense, though the MBH accretes a slightly higher fraction of cold flow gas.

edges support from The Grainger Foundation. The authors thank Kelly Holley-Bockelmann, Ferah Munshi, and the anonymous referee for their helpful comments.

REFERENCES

- Abel, T., Bryan, G. L., & Norman, M. L. 2002, *Science*, 295, 93
 Alexander, D. M., Smail, I., Bauer, F. E., Chapman, S. C., Blain, A. W., Brandt, W. N., & Ivison, R. J. 2005, *Nature*, 434, 738
 Bahcall, J. N., Kirhakos, S., Saxe, D. H., & Schneider, D. P. 1997, *ApJ*, 479, 642
 Begelman, M. C., Volonteri, M., & Rees, M. J. 2006, *MNRAS*, 370, 289
 Bellovary, J., Volonteri, M., Governato, F., Shen, S., Quinn, T., & Wadsley, J. 2011, *ApJ*, 742, 13

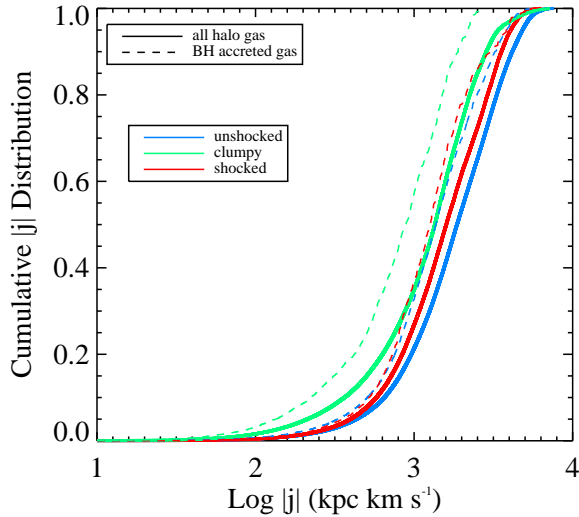


FIG. 8.— Normalized cumulative distribution of the log of specific angular momentum of gas at the moment it enters the main galaxy in simulation *hz2*. Colors are as in Figure 5. Dashed lines represent all of the gas that enters the main galaxy; solid lines indicate only that gas which is eventually accreted by the central MBH. For each mode of accretion, the gas which is accreted by the MBH has lower angular momentum than the galaxy as a whole.

Bellovary, J. M., Governato, F., Quinn, T. R., Wadsley, J., Shen, S., & Volonteri, M. 2010, *ApJL*, 721, L148
 Bennert, N., Canalizo, G., Jungwiert, B., Stockton, A., Schweizer, F., Peng, C. Y., & Lacy, M. 2008, *ApJ*, 677, 846
 Benson, A. J. 2005, *MNRAS*, 358, 551
 Binney, J. 1977, *ApJ*, 215, 483
 Bower, R. G., Benson, A. J., Malbon, R., Helly, J. C., Frenk, C. S., Baugh, C. M., Cole, S., & Lacey, C. G. 2006, *MNRAS*, 370, 645
 Bromm, V., Ferrara, A., Coppi, P. S., & Larson, R. B. 2001, *MNRAS*, 328, 969
 Bromm, V., & Larson, R. B. 2004, *ARA&A*, 42, 79
 Brook, C. B. et al. 2011, *MNRAS*, 415, 1051
 Brooks, A. M., Governato, F., Booth, C. M., Willman, B., Gardner, J. P., Wadsley, J., Stinson, G., & Quinn, T. 2007, *ApJL*, 655, L17
 Brooks, A. M., Governato, F., Quinn, T., Brook, C. B., & Wadsley, J. 2009, *ApJ*, 694, 396
 Brooks, A. M. et al. 2011, *ApJ*, 728, 51
 Canalizo, G., & Stockton, A. 2001, *ApJ*, 555, 719
 Chen, C.-T. J. et al. 2013, *ApJ*, 773, 3
 Christensen, C., Governato, F., Quinn, T., Brooks, A. M., Fisher, D. B., Shen, S., McCleary, J., & Wadsley, J. 2012, *ArXiv e-prints*
 Coppin, K. et al. 2010, *ApJ*, 713, 503
 Couchman, H. M. P., & Rees, M. J. 1986, *MNRAS*, 221, 53
 Danovich, M., Dekel, A., Hahn, O., & Teyssier, R. 2012, *MNRAS*, 422, 1732
 De Robertis, M. M., Yee, H. K. C., & Hayhoe, K. 1998, *ApJ*, 496, 93
 Dekel, A., & Birnboim, Y. 2006, *MNRAS*, 368, 2
 Dekel, A. et al. 2009, *Nature*, 457, 451
 Di Matteo, T., Colberg, J., Springel, V., Hernquist, L., & Sijacki, D. 2008, *ApJ*, 676, 33
 Di Matteo, T., Khandai, N., DeGraf, C., Feng, Y., Croft, R. A. C., Lopez, J., & Springel, V. 2012, *ApJL*, 745, L29
 Di Matteo, T., Springel, V., & Hernquist, L. 2005, *Nature*, 433, 604
 Disney, M. J. et al. 1995, *Nature*, 376, 150
 Dubois, Y., Pichon, C., Devriendt, J., Silk, J., Haehnelt, M., Kimm, T., & Slyz, A. 2013, *MNRAS*, 428, 2885
 Dubois, Y., Pichon, C., Haehnelt, M., Kimm, T., Slyz, A., Devriendt, J., & Pogosyan, D. 2012, *MNRAS*, 423, 3616
 Eisenstein, D. J., & Loeb, A. 1995, *ApJ*, 443, 11
 García-Burillo, S., Combes, F., Schinnerer, E., Boone, F., & Hunt, L. K. 2005, *AAP*, 441, 1011

Gill, S. P. D., Knebe, A., & Gibson, B. K. 2004, *MNRAS*, 351, 399
 Governato, F. et al. 2010, *Nature*, 463, 203
 —. 2009, *MNRAS*, 398, 312
 Gross, M. A. K. 1997, PhD thesis, UNIVERSITY OF CALIFORNIA, SANTA CRUZ
 Guedes, J., Callegari, S., Madau, P., & Mayer, L. 2011, *ApJ*, 742, 76
 Gültekin, K. et al. 2009, *ApJ*, 698, 198
 Guyon, O., Sanders, D. B., & Stockton, A. 2006, *ApJS*, 166, 89
 Haan, S., Schinnerer, E., Emsellem, E., García-Burillo, S., Combes, F., Mundell, C. G., & Rix, H. 2009, *ApJ*, 692, 1623
 Haardt, F., & Madau, P. 1996, *ApJ*, 461, 20
 Haiman, Z., & Loeb, A. 2001, *ApJ*, 552, 459
 Hicks, E. K. S., Davies, R. I., Maciejewski, W., Emsellem, E., Malkan, M. A., Dumas, G., Müller-Sánchez, F., & Rivers, A. 2013, *ApJ*, 768, 107
 Hopkins, A. M. 2004, *ApJ*, 615, 209
 Hopkins, P. F., Hernquist, L., Cox, T. J., Di Matteo, T., Robertson, B., & Springel, V. 2006, *ApJS*, 163, 1
 Hutchings, J. B., Maddox, N., Cutri, R. M., & Nelson, B. O. 2003, *AJ*, 126, 63
 Jonsson, P. 2006, *MNRAS*, 372, 2
 Katz, N. 1992, *ApJ*, 391, 502
 Kauffmann, G., & Haehnelt, M. 2000, *MNRAS*, 311, 576
 Kereš, D., Katz, N., Fardal, M., Davé, R., & Weinberg, D. H. 2009, *MNRAS*, 395, 160
 Kereš, D., Katz, N., Weinberg, D. H., & Davé, R. 2005, *MNRAS*, 363, 2
 Kimm, T., Devriendt, J., Slyz, A., Pichon, C., Kassin, S. A., & Dubois, Y. 2011, *ArXiv e-prints*
 Kirkpatrick, A. et al. 2012, *ApJ*, 759, 139
 Knebe, A., Green, A., & Binney, J. 2001, *MNRAS*, 325, 845
 Knollmann, S. R., & Knebe, A. 2009, *ApJS*, 182, 608
 Kocevski, D. D. et al. 2012, *ApJ*, 744, 148
 Koushiappas, S. M., Bullock, J. S., & Dekel, A. 2004, *MNRAS*, 354, 292
 Kroupa, P. 2001, *MNRAS*, 322, 231
 Li, Y. et al. 2007, *ApJ*, 665, 187
 Lodato, G., & Natarajan, P. 2006, *MNRAS*, 371, 1813
 Loeb, A., & Rasio, F. A. 1994, *ApJ*, 432, 52
 McKee, C. F., & Ostriker, J. P. 1977, *ApJ*, 218, 148
 Menéndez-Delmestre, K. et al. 2007, *ApJL*, 655, L65
 Moster, B. P., Somerville, R. S., Maulbetsch, C., van den Bosch, F. C., Macciò, A. V., Naab, T., & Oser, L. 2010, *ApJ*, 710, 903
 Mullaney, J. R. et al. 2012, *MNRAS*, 419, 95
 Munshi, F. et al. 2013, *ApJ*, 766, 56
 Ocvirk, P., Pichon, C., & Teyssier, R. 2008, *MNRAS*, 390, 1326
 Papovich, C. et al. 2006, *ApJ*, 640, 92
 Pichon, C., Pogosyan, D., Kimm, T., Slyz, A., Devriendt, J., & Dubois, Y. 2011, *MNRAS*, 418, 2493
 Reddy, N. A., Steidel, C. C., Pettini, M., Adelberger, K. L., Shapley, A. E., Erb, D. K., & Dickinson, M. 2008, *ApJS*, 175, 48
 Richards, G. T. et al. 2006, *AJ*, 131, 2766
 Roškar, R., Debattista, V. P., Brooks, A. M., Quinn, T. R., Brook, C. B., Governato, F., Dalcanton, J. J., & Wadsley, J. 2010, *MNRAS*, 408, 783
 Ryan, C. J., De Robertis, M. M., Virani, S., Laor, A., & Dawson, P. C. 2007, *ApJ*, 654, 799
 Sanders, D. B., Soifer, B. T., Elias, J. H., Madore, B. F., Matthews, K., Neugebauer, G., & Scoville, N. Z. 1988, *ApJ*, 325, 74
 Schawinski, K., Dowlin, N., Thomas, D., Urry, C. M., & Edmondson, E. 2010, *ApJL*, 714, L108
 Schawinski, K., Treister, E., Urry, C. M., Cardamone, C. N., Simmons, B., & Yi, S. K. 2011, *ApJL*, 727, L31
 Shen, S., Wadsley, J., & Stinson, G. 2010, *MNRAS*, 407, 1581
 Sijacki, D., Springel, V., di Matteo, T., & Hernquist, L. 2007, *MNRAS*, 380, 877
 Sijacki, D., Springel, V., & Haehnelt, M. G. 2009, *MNRAS*, 400, 100
 Silverman, J. D. et al. 2011, *ApJ*, 743, 2
 —. 2009, *ApJ*, 696, 396
 Spergel, D. N. et al. 2007, *ApJS*, 170, 377
 Stadel, J. G. 2001, PhD thesis, AA(UNIVERSITY OF WASHINGTON)

- Stewart, K. R., Brooks, A. M., Bullock, J. S., Maller, A. H., Diemand, J., Wadsley, J., & Moustakas, L. A. 2013, *ApJ*, 769, 74
- Stewart, K. R., Kaufmann, T., Bullock, J. S., Barton, E. J., Maller, A. H., Diemand, J., & Wadsley, J. 2011, *ApJL*, 735, L1
- Stinson, G., Seth, A., Katz, N., Wadsley, J., Governato, F., & Quinn, T. 2006, *MNRAS*, 373, 1074
- Tal, T., van Dokkum, P. G., Nelan, J., & Bezanson, R. 2009, *AJ*, 138, 1417
- Tillson, H., Devriendt, J., Slyz, A., Miller, L., & Pichon, C. 2012, *ArXiv e-prints*
- Treister, E., Schawinski, K., Urry, C. M., & Simmons, B. D. 2012, *ApJL*, 758, L39
- Urrutia, T., Lacy, M., & Becker, R. H. 2008, *ApJ*, 674, 80
- van de Voort, F., Schaye, J., Booth, C. M., Haas, M. R., & Dalla Vecchia, C. 2011, *MNRAS*, 414, 2458
- Van Wassenhove, S., Volonteri, M., Mayer, L., Dotti, M., Bellovary, J., & Callegari, S. 2012, *ApJL*, 748, L7
- Volonteri, M., & Natarajan, P. 2009, *MNRAS*, 400, 1911
- Wadsley, J. W., Stadel, J., & Quinn, T. 2004, *New Astronomy*, 9, 137
- Wolf, M. J., & Sheinis, A. I. 2008, *AJ*, 136, 1587